

Factorized time correlation diagram analysis of paired causal systems excited by twin stochastic driving functions

Daniel P. Biebighauser, Daniel B. Turner, and Darin J. Ulness
Department of Chemistry, Concordia College, Moorhead, Minnesota 56562
 (Received 11 July 2001; published 25 January 2002)

This work examines the properties and mathematical structure of factorized time correlation (FTC) diagram analysis in a general context. The goal is to extract general principles and analytic behavior that are not tied to any particular phenomenon in physics. It is hoped that this will provide a basis for expanded use of FTC diagram analysis beyond its current employment in the study of noisy light-based nonlinear optical spectroscopy. Furthermore, the concept of indirect correlation in a two-channel system driven by twin stationary circular Gaussian stochastic inputs is defined and discussed both analytically and through FTC diagram analysis.

DOI: 10.1103/PhysRevE.65.026142

PACS number(s): 05.10.Gg, 02.50.Fz, 02.70.Rr

I. INTRODUCTION

Stochastic (random) processes are ubiquitous in all branches of science. Often one is concerned with the case where such stochastic processes serve as “inputs” to a deterministic causal system to produce a stochastic “output.” Such a system is characterized by its (in general, nonlinear) response function. Numerous references exist on the subject of stationary random functions (see, for example [1]) and the nonlinear transformations of such functions [2,3]. Often, one takes some sort of perturbation theory approach to these types of problems. The perturbation series is based on the number of times the driving function acts on the system. Thus, in the standard way, one obtains a series of successively higher-order integral equations which must be solved.

In the current paper, factorized time correlation (FTC) diagram analysis [4–10] is applied to a special case in which the “input” stochastic function is a superposition of a stationary Gaussian random function [11,12] and its displaced (time-delayed) “twin.” FTC diagram analysis is a technique used to determine the properties of material system-response functions (which are deterministic and causal) by using stochastic perturbations of the system. The basic system is comprised of two channels (1 and 2) each having a (in general, different) nonlinear response. The system is taken to be stationary as well. That is, the response of the system is invariant with respect to absolute time. The two “outputs” are multiplied together and stochastically averaged. We are interested in this average as a function of the time delay between the twin input functions. The primary focus of this paper is on the second-order/second-order case (to be described in detail below) because this is the lowest order in which the very interesting phenomenon of indirect correlation arises. Indirect correlation has only been briefly discussed in the literature within the context of nonlinear optical spectroscopy [5]. The extension to higher orders is straightforward and does not pose any fundamental difficulties. The primary motivation for dealing specifically with the second-order/second-order case rather than taking a more general n_1^{th} -order/ n_2^{th} -order case approach is to give concreteness to the mathematical basis of FTC diagram analysis and to the

accompanying physical “tools” associated with the FTC diagrams.

This two-channel stationary model has applications in situations where fluctuating amplitude responses are quadrature (intensity level) detected and averaged; obvious examples being in optics, spectroscopy, electronics, and signal processing. FTC diagram analysis of this type of system is currently a useful tool in analyzing certain problems that arise in nonlinear optical spectroscopy. In fact, FTC diagram analysis was invented specifically to attack the theoretical challenges of noisy light-based nonlinear optical spectroscopy [4]. FTC diagram analysis of noisy light spectroscopy has provided great physical insight along with computational advantage [4–10]. This paper is a discussion of FTC diagram analysis outside of the context of noisy light spectroscopy. The goal is to fully abstract the mathematical methodology of FTC diagram analysis away from any particular physical problem (e.g., from noisy light spectroscopy). With this accomplished, it is hoped that FTC diagram analysis might find use in future work involving physical phenomena far removed from noisy light spectroscopy, such that it might serve as a common method that links distinct physical phenomena. Such a link might provide fruitful cross fertilization of ideas and approaches that could be very beneficial to the study of both noisy light and other phenomena.

II. RESPONSE OF THE TWO-CHANNEL SYSTEM

The input for channel 1, $V(t)$, of the two-channel system is a superposition of two stochastic functions $F(t)$ and $F'(t) \equiv F(t - \tau)$ [i.e., $F'(t)$ is “delayed” with respect to $F(t)$ by an amount τ]. That is, $V(t) = F(t) + F'(t)$. The stochastic function $F(t)$ is taken to be a stationary circular Gaussian random function of time with its mean equal to zero. Channel 2 also has input $V(s)$ (throughout this paper, the variable s will be used for time for channel 2 to clearly distinguish it from channel 1). The deterministic stationary nonlinear response function of channel 1 (channel 2) is $R_1(R_2)$. The output “amplitude,” $A_1(t, \tau)$ [$A_2(s, \tau)$] of channel 1 (channel 2) remains a stationary random function of time. One is interested in the stochastic average of the product of outputs from the two channels:

TABLE I. The four-point time correlation functions that arise from multiplying out the right-hand side of Eq. (6). The 16 terms are arbitrarily identified by a capital roman numeral (I-VIII) and a lower case letter (a or b) for ease of referral in the text.

Term	a	b
I	$\langle F(t'_2)F(t'_1)F(s'_1)F(s'_2) \rangle$	$\langle F(t'_2 - \tau)F(t'_1)F(s'_1)F(s'_2) \rangle$
II	$\langle F(t'_2)F(t'_1 - \tau)F(s'_1)F(s'_2) \rangle$	$\langle F(t'_2 - \tau)F(t'_1 - \tau)F(s'_1)F(s'_2) \rangle$
III	$\langle F(t'_2)F(t'_1)F(s'_1 - \tau)F(s'_2) \rangle$	$\langle F(t'_2 - \tau)F(t'_1)F(s'_1 - \tau)F(s'_2) \rangle$
IV	$\langle F(t'_2)F(t'_1 - \tau)F(s'_1 - \tau)F(s'_2) \rangle$	$\langle F(t'_2 - \tau)F(t'_1 - \tau)F(s'_1 - \tau)F(s'_2) \rangle$
V	$\langle F(t'_2)F(t'_1)F(s'_1)F(s'_2 - \tau) \rangle$	$\langle F(t'_2 - \tau)F(t'_1)F(s'_1)F(s'_2 - \tau) \rangle$
VI	$\langle F(t'_2)F(t'_1 - \tau)F(s'_1)F(s'_2 - \tau) \rangle$	$\langle F(t'_2 - \tau)F(t'_1 - \tau)F(s'_1)F(s'_2 - \tau) \rangle$
VII	$\langle F(t'_2)F(t'_1)F(s'_1 - \tau)F(s'_2 - \tau) \rangle$	$\langle F(t'_2 - \tau)F(t'_1)F(s'_1 - \tau)F(s'_2 - \tau) \rangle$
VIII	$\langle F(t'_2)F(t'_1 - \tau)F(s'_1 - \tau)F(s'_2 - \tau) \rangle$	$\langle F(t'_2 - \tau)F(t'_1 - \tau)F(s'_1 - \tau)F(s'_2 - \tau) \rangle$

$$I(t-s; \tau) = \langle A_2(s, \tau)A_1(t, \tau) \rangle. \quad (1)$$

Since the amplitudes are stationary functions, only the difference between t and s is of importance. The special case of $t=s$ is particularly important because it represents a direct time-average “intensity” measurement. For example, in optics, this would represent light intensity at a point in space, and in spectroscopy this would represent homodyne detection of the signal.

It is not feasible to derive a completely closed form for $A_1(t, \tau)$ and $A_2(s, \tau)$ given a fully general stationary response function. Instead here, we assume A_1 (and A_2) may be expanded in a perturbation series based on the number (n_i) of times channel 1 (channel 2) samples the input: $A_1(t, \tau) = \sum_{n_1} A_1^{(n_1)}(t, \tau)$ ($A_2(t, \tau) = \sum_{n_2} A_2^{(n_2)}(t, \tau)$). That is, we assume that the contribution to A_1 (and A_2) decreases sufficiently rapidly as a function of the number of samplings of the input, such that it is well approximated by the low-order terms. Furthermore, each successive order introduces smaller corrections to A_1 (and A_2) than the previous order.

III. THE SECOND-ORDER/SECOND-ORDER CASE

The second-order/second-order case of the general development outlined above is taken as the working example. By second-order/second-order, it is meant that $A_1(t, \tau) = A_1^{(2)}(t, \tau)$ and $A_2(s, \tau) = A_2^{(2)}(s, \tau)$. Thus, the main goal will be the evaluation of $\langle A_2^{(2)}(s, \tau)A_1^{(2)}(t, \tau) \rangle$. As stated above, the order gives the number of times the random input, $V(t)$, acts on the system (in a perturbative sense). Consequently,

$$A_1^{(2)}(t, \tau) = \int_{-\infty}^t dt'_2 \int_{-\infty}^{t'_2} dt'_1 R_1(t-t'_2; t'_2-t'_1) V(t'_2) V(t'_1). \quad (2)$$

This expression states that $V(t)$ first acts at time $t=t'_1$ whereupon the system propagates according to the response function R_1 until $V(t)$ acts for the second time at $t=t'_2$. The system then propagates until the time t . In general, the response during the interval $t'_2-t'_1$ is different than during the interval $t-t'_2$. The output amplitude for channel 2 is similarly

$$A_2^{(2)}(s, \tau) = \int_{-\infty}^s ds'_2 \int_{-\infty}^{s'_2} ds'_1 R_2(s-s'_2; s'_2-s'_1) V(s'_2) V(s'_1), \quad (3)$$

where again distinct time variables from that of channel 1 are required.

Evaluation of $\langle A_2^{(2)}(s, \tau)A_1^{(2)}(t, \tau) \rangle$ proceeds as follows:

$$\begin{aligned} & \langle A_2^{(2)}(s, \tau)A_1^{(2)}(t, \tau) \rangle \\ &= \left\langle \int_{-\infty}^t dt'_2 \int_{-\infty}^{t'_2} dt'_1 \int_{-\infty}^s ds'_2 \int_{-\infty}^{s'_2} ds'_1 R_1(t-t'_2; t'_2-t'_1) \right. \\ & \quad \left. \times R_2(s-s'_2; s'_2-s'_1) V(t'_2) V(t'_1) V(s'_2) V(s'_1) \right\rangle, \quad (4) \end{aligned}$$

The R 's are deterministic so the averaging operation can be brought inside the integration and applied only to the V 's.

$$\begin{aligned} & \langle A_2^{(2)}(s, \tau)A_1^{(2)}(t, \tau) \rangle \\ &= \int_{-\infty}^t dt'_2 \int_{-\infty}^{t'_2} dt'_1 \int_{-\infty}^s ds'_2 \int_{-\infty}^{s'_2} ds'_1 R_1(t-t'_2; t'_2-t'_1) \\ & \quad \times R_2(s-s'_2; s'_2-s'_1) \langle V(t'_2) V(t'_1) V(s'_2) V(s'_1) \rangle. \quad (5) \end{aligned}$$

Now, the random driving function can be written more explicitly as $V = F + F'$. So, the $\langle V(t'_2) V(t'_1) V(s'_2) V(s'_1) \rangle$ factor in Eq. (5) becomes

$$\begin{aligned} & \langle V(t'_2) V(t'_1) V(s'_2) V(s'_1) \rangle \\ &= \left\langle [F(t'_2) + F(t'_2 - \tau)][F(t'_1) + F(t'_1 - \tau)] \right. \\ & \quad \left. \times [F(s'_2) + F(s'_2 - \tau)][F(s'_1) + F(s'_1 - \tau)] \right\rangle. \quad (6) \end{aligned}$$

The right-hand side is multiplied out to give 16 terms which are collected in Table I. Each of these terms is a *four-point time correlation function*.

For concreteness, we consider one of these 16 terms as an example; term VIa: $\langle F(t'_2)F(t'_1 - \tau)F(s'_1)F(s'_2 - \tau) \rangle$. For this choice, the appropriate term from Eq. (5) is

TABLE II. The 48 products of pair correlators arising from applying the Gaussian moment theorem to the four-point time correlation functions of Table I.

Term	i	ii	iii
Ia	$\langle F(t'_1)F(t'_2)\rangle\langle F(s'_2)F(s'_1)\rangle$	$\langle F(s'_1)F(t'_2)\rangle\langle F(s'_2)F(t'_1)\rangle$	$\langle F(s'_2)F(t'_2)\rangle\langle F(s'_1)F(t'_1)\rangle$
Ib	$\langle F(t'_1)F(t'_2-\tau)\rangle\langle F(s'_2)F(s'_1)\rangle$	$\langle F(s'_1)F(t'_2-\tau)\rangle\langle F(s'_2)F(t'_1)\rangle$	$\langle F(s'_2)F(t'_2-\tau)\rangle\langle F(s'_1)F(t'_1)\rangle$
IIa	$\langle F(t'_1-\tau)F(t'_2)\rangle\langle F(s'_2)F(s'_1)\rangle$	$\langle F(s'_1)F(t'_2)\rangle\langle F(s'_2)F(t'_1-\tau)\rangle$	$\langle F(s'_2)F(t'_2)\rangle\langle F(s'_1)F(t'_1-\tau)\rangle$
IIb	$\langle F(t'_1-\tau)F(t'_2-\tau)\rangle\langle F(s'_2)F(s'_1)\rangle$	$\langle F(s'_1)F(t'_2-\tau)\rangle\langle F(s'_2)F(t'_1-\tau)\rangle$	$\langle F(s'_2)F(t'_2-\tau)\rangle\langle F(s'_1)F(t'_1-\tau)\rangle$
IIIa	$\langle F(t'_1)F(t'_2)\rangle\langle F(s'_2)F(s'_1-\tau)\rangle$	$\langle F(s'_1-\tau)F(t'_2)\rangle\langle F(s'_2)F(t'_1)\rangle$	$\langle F(s'_2)F(t'_2)\rangle\langle F(s'_1-\tau)F(t'_1)\rangle$
IIIb	$\langle F(t'_1)F(t'_2-\tau)\rangle\langle F(s'_2)F(s'_1-\tau)\rangle$	$\langle F(s'_1-\tau)F(t'_2-\tau)\rangle\langle F(s'_2)F(t'_1)\rangle$	$\langle F(s'_2)F(t'_2-\tau)\rangle\langle F(s'_1-\tau)F(t'_1)\rangle$
IVa	$\langle F(t'_1-\tau)F(t'_2)\rangle\langle F(s'_2)F(s'_1-\tau)\rangle$	$\langle F(s'_1-\tau)F(t'_2)\rangle\langle F(s'_2)F(t'_1-\tau)\rangle$	$\langle F(s'_2)F(t'_2)\rangle\langle F(s'_1-\tau)F(t'_1-\tau)\rangle$
IVb	$\langle F(t'_1-\tau)F(t'_2-\tau)\rangle\langle F(s'_2)F(s'_1-\tau)\rangle$	$\langle F(s'_1-\tau)F(t'_2-\tau)\rangle\langle F(s'_2)F(t'_1-\tau)\rangle$	$\langle F(s'_2)F(t'_2-\tau)\rangle\langle F(s'_1-\tau)F(t'_1-\tau)\rangle$
Va	$\langle F(t'_1)F(t'_2)\rangle\langle F(s'_2-\tau)F(s'_1)\rangle$	$\langle F(s'_1)F(t'_2)\rangle\langle F(s'_2-\tau)F(t'_1)\rangle$	$\langle F(s'_2-\tau)F(t'_2)\rangle\langle F(s'_1)F(t'_1)\rangle$
Vb	$\langle F(t'_1)F(t'_2-\tau)\rangle\langle F(s'_2-\tau)F(s'_1)\rangle$	$\langle F(s'_1)F(t'_2-\tau)\rangle\langle F(s'_2-\tau)F(t'_1)\rangle$	$\langle F(s'_2-\tau)F(t'_2-\tau)\rangle\langle F(s'_1)F(t'_1)\rangle$
VIa	$\langle F(t'_1-\tau)F(t'_2)\rangle\langle F(s'_2-\tau)F(s'_1)\rangle$	$\langle F(s'_1)F(t'_2)\rangle\langle F(s'_2-\tau)F(t'_1-\tau)\rangle$	$\langle F(s'_2-\tau)F(t'_2)\rangle\langle F(s'_1)F(t'_1-\tau)\rangle$
VIb	$\langle F(t'_1-\tau)F(t'_2-\tau)\rangle\langle F(s'_2-\tau)F(s'_1)\rangle$	$\langle F(s'_1)F(t'_2-\tau)\rangle\langle F(s'_2-\tau)F(t'_1-\tau)\rangle$	$\langle F(s'_2-\tau)F(t'_2-\tau)\rangle\langle F(s'_1)F(t'_1-\tau)\rangle$
VIIa	$\langle F(t'_1)F(t'_2)\rangle\langle F(s'_2-\tau)F(s'_1-\tau)\rangle$	$\langle F(s'_1-\tau)F(t'_2)\rangle\langle F(s'_2-\tau)F(t'_1)\rangle$	$\langle F(s'_2-\tau)F(t'_2)\rangle\langle F(s'_1-\tau)F(t'_1)\rangle$
VIIb	$\langle F(t'_1)F(t'_2-\tau)\rangle\langle F(s'_2-\tau)F(s'_1-\tau)\rangle$	$\langle F(s'_1-\tau)F(t'_2-\tau)\rangle\langle F(s'_2-\tau)F(t'_1)\rangle$	$\langle F(s'_2-\tau)F(t'_2-\tau)\rangle\langle F(s'_1-\tau)F(t'_1)\rangle$
VIIIa	$\langle F(t'_1-\tau)F(t'_2)\rangle\langle F(s'_2-\tau)F(s'_1-\tau)\rangle$	$\langle F(s'_1-\tau)F(t'_2)\rangle\langle F(s'_2-\tau)F(t'_1-\tau)\rangle$	$\langle F(s'_2-\tau)F(t'_2)\rangle\langle F(s'_1-\tau)F(t'_1-\tau)\rangle$
VIIIb	$\langle F(t'_1-\tau)F(t'_2-\tau)\rangle\langle F(s'_2-\tau)F(s'_1-\tau)\rangle$	$\langle F(s'_1-\tau)F(t'_2-\tau)\rangle\langle F(s'_2-\tau)F(t'_1-\tau)\rangle$	$\langle F(s'_2-\tau)F(t'_2-\tau)\rangle\langle F(s'_1-\tau)F(t'_1-\tau)\rangle$

$$\begin{aligned}
& \langle A_2^{(2)}(s, \tau)A_1^{(2)}(t, \tau) \rangle \\
&= \int_{-\infty}^t dt'_2 \int_{-\infty}^{t'_2} dt'_1 \int_{-\infty}^s ds'_2 \int_{-\infty}^{s'_2} ds'_1 R_1(t-t'_2; t'_2-t'_1) \\
& \quad \times R_2(s-s'_2; s'_2-s'_1) \langle F(t'_2)F(t'_1-\tau)F(s'_1)F(s'_2-\tau) \rangle. \quad (7)
\end{aligned}$$

The four-point time correlation function in this equation cannot be evaluated conveniently unless we assume the random functions F obey *circular Gaussian statistics*. With this assumption, all the four-point time correlators can be factorized into a (three-term) sum of a product of (two) two-point correlators according to the Gaussian moment theorem [11–13]. Ultimately, this results in $16 \times 3 = 48$ terms (Table II). Applying the Gaussian moment theorem to term VIa one obtains

$$\begin{aligned}
& \langle F(t'_2)F(t'_1-\tau)F(s'_1)F(s'_2-\tau) \rangle \\
&= \langle F(t'_1-\tau)F(t'_2) \rangle \langle F(s'_2-\tau)F(s'_1) \rangle \quad (i) \quad (8) \\
&+ \langle F(s'_1)F(t'_2) \rangle \langle F(s'_2-\tau)F(t'_1-\tau) \rangle \quad (ii) \\
&+ \langle F(s'_2-\tau)F(t'_2) \rangle \langle F(s'_1)F(t'_1-\tau) \rangle. \quad (iii)
\end{aligned}$$

In the next section, these terms will be evaluated using FTC diagram analysis, but now, for completeness, we shall evaluate one of these terms analytically. Focusing on term T_{VIa} , one needs to evaluate

$$\begin{aligned}
T_{\text{VIa}} &= \int_{-\infty}^t dt'_2 \int_{-\infty}^{t'_2} dt'_1 \int_{-\infty}^s ds'_2 \int_{-\infty}^{s'_2} ds'_1 R_1(t-t'_2; t'_2-t'_1) \\
& \quad \times R_2(s-s'_2; s'_2-s'_1) \langle F(s'_2-\tau)F(t'_2) \rangle \\
& \quad \times \langle F(s'_1)F(t'_1-\tau) \rangle. \quad (9)
\end{aligned}$$

It is convenient to make the change of variables $t=t$, $t_2=t-t'_2$, $t_1=t'_2-t'_1$, $s=s$, $s_2=s-s'_2$, $s_1=s'_2-s'_1$. (Note that upon this change of variables t_2 , t_1 , s_2 , and s_1 represent time intervals rather than times of action by the random driving function.) This gives

$$\begin{aligned}
T_{\text{VIa}} &= \int_0^\infty dt_2 \int_0^\infty dt_1 \int_0^\infty ds_2 \int_0^\infty ds_1 R_1(t_2; t_1) R_2(s_2; s_1) \\
& \quad \times \langle F(t-t_2)F(s-s_2-\tau) \rangle \langle F(t-t_2-t_1-\tau) \rangle \\
& \quad \times F(s-s_2-s_1). \quad (10)
\end{aligned}$$

If F is white, i.e., if it is completely random, then $\langle F(a)F(b) \rangle = \delta(a-b)$, where δ is the Dirac δ function. So,

$$\begin{aligned}
T_{\text{VIa}} &= \int_0^\infty dt_2 \int_0^\infty dt_1 \int_0^\infty ds_2 \int_0^\infty ds_1 R_1(t_2; t_1) R_2(s_2; s_1) \\
& \quad \times \delta(t-t_2-s+s_2+\tau) \delta(t-t_2-t_1-\tau-s+s_2+s_1). \quad (11)
\end{aligned}$$

Performing the s_1 integration gives

$$\begin{aligned}
T_{\text{VIa}} &= \int_0^\infty dt_2 \int_0^\infty dt_1 \int_0^\infty ds_2 R_1(t_2; t_1) R_2(s_2; -t+t_2+t_1+\tau \\
& \quad +s-s_2) \delta(t-t_2-s+s_2+\tau), \quad (12)
\end{aligned}$$

and performing the s_2 integration gives

TABLE III. The FTC diagrams derived from the 48 terms in Table II.

Term	ai	aii	aiii	bi	bii	biii
I						
II						
III						
IV						
V						
VI						
VII						
VIII						

$$T_{VIaiii} = \int_0^\infty dt_2 \int_0^\infty dt_1 R_1(t_2; t_1) R_2(s - t + t_2 - \tau; t_1 + 2\tau). \tag{13}$$

This is the general form (restricted by our above assumptions). A causal R is implied from the initial definition. (Implications of causality in R are discussed in more detail in Appendix A.) For the very common case when $s = t$, Eq. (13) simplifies to

$$T_{VIaiii} = \int_0^\infty dt_2 \int_0^\infty dt_1 R_1(t_2; t_1) R_2(t_2 - \tau; t_1 + 2\tau). \tag{14}$$

IV. FTC DIAGRAMS

It is convenient to represent the factorized terms in Eq. (10) pictorially as FTC diagrams. The FTC diagrams and FTC diagram analysis provide a general mechanism for translating the initial expressions to their evaluated form. In general, a FTC diagram, representing a n_1^{th} -order/ n_2^{th} -order

factorized time correlator, consists of a template having two horizontal timelines t and s which represent channels 1 and 2, respectively. Superimposed on each of these timelines are n_1 and n_2 tick marks—one for each time integration variable $\{t'_i\}$ and $\{s'_i\}$. For the second-order/second-order case studied here, each line then has two tick marks. A single FTC diagram can be constructed for each term in Table II and these diagrams are collected in Table III. Factors (pair correlators) of the form $\langle F(a)F(b) \rangle$, where a and b are any given time variable, and $\langle F'(a)F'(b) \rangle = \langle F(a - \tau)F(b - \tau) \rangle$, which can be written as $\langle F(a)F(b) \rangle$ under stationarity, are τ independent. Such terms are represented in the FTC diagrams by a *line* segment connecting the two time points involved in the pair correlator. Factors of the form $\langle F'(a)F(b) \rangle$ and $\langle F(a)F'(b) \rangle$ are τ dependent and are represented by *arrow* segments drawn from the tick mark corresponding to the time argument of F to the tick mark corresponding to the time argument of F' . So, in Table III, 12 of the 48 FTC diagrams represent completely τ -independent terms. These diagrams are $T_{Iai-iii}$, T_{IIbi} , T_{IIIbii} , T_{IVaiii} , T_{Vbiii} , T_{VIaii} , T_{VIIai} , and $T_{VIIIbi-iii}$. The remaining 36 diagrams are

τ dependent and contribute to the “interesting” features of the signal. They probe the dynamics of the system.

Any pair correlator (line or arrow segment in the FTC diagram) represents the *direct correlation* between actions of the driving function. With the appropriate normalization, the pair correlator is unity when the difference in the time arguments is zero and it vanishes as the difference in the time arguments tends to infinity. The rate at which the pair correlator vanishes from unity is characterized by the correlation time τ_c of the stochastic process. A precise definition of τ_c is not needed for this paper—only that the pair correlator is appreciable for time differences smaller than τ_c and is negligible for time differences greater than τ_c . Since one of the primary interests of this paper is demonstrating *indirect correlation*, which can be much greater than τ_c , we shall make the simplifying (but not required) approximation that $\tau_c \rightarrow 0$, i.e., the pair correlators can be replaced with δ functions. This is the same assumption that was used in the previous section to provide the δ functions that assisted the integration during the analytic calculation.

Associated with FTC diagram analysis are several primary principles or “tools.” We shall show that indirect correlation follows as a “secondary” principle from two primary principles of FTC diagram analysis—namely, *synchronization* and *accumulation* (now to be discussed in turn). Synchronization and accumulation act together to determine the relative strength of the terms represented diagrammatically by the FTC diagrams.

A. Synchronization

Any given pair correlator “synchronizes” its two time arguments to within roughly τ_c (otherwise the correlator vanishes). Under our current approximation of a δ -function correlator ($\tau_c = 0$), the two time arguments are exactly synchronized. For example, the pair correlator $\langle F(s_i)F(t_j) \rangle$ forces t_j (on the t timeline) to be coincident with s_i (on the s timeline). Likewise the pair correlator $\langle F'(s_k)F(t_l) \rangle = \langle F(s_k - \tau)F(t_l) \rangle$ forces t_l to be coincident with $s_k - \tau$.

The system response function can serve to soften the synchronization condition on a single timeline (*intrachannel*). That is, for any noninstantaneous response function, a given channel of the system carries a “memory” of the stochastic input. This memory can allow for the direct correlation between the time arguments to be longer than τ_c and characterized by the decay of the system memory. And this type of synchronization allows for a direct measurement of the system response function. The FTC diagrams in columns ai and bi that contain at least one arrow segment allow for the direct probing of the system since the independent pair correlators are intrachannel.

The majority of the FTC diagrams in Table III do not contain intrachannel correlations, however. The FTC diagrams in columns aii, aiii, bii, and biii contain only *interchannel* correlations, since all the line and arrow segments connect a tick mark on the t timeline to a tick mark on the s timeline. At first glance, it appears that these diagrams would be of little interest because it would seem that these correlations do not probe the system response function. As we shall

shortly see, however, these diagrams are important (and, in fact, dominant in many situations) because of *indirect correlation*. Before addressing indirect correlation more thoroughly, we must first discuss the idea of accumulation.

B. Accumulation

Since the inputs F and F' are infinitely extended functions of time, they may be sampled by the system at any time. This point is represented analytically by the time-ordered integrals appearing in the expressions for $A_1^{(2)}(t)$ and $A_2^{(2)}(s)$ [Eqs. (2) and (3)]. In terms of the FTC diagrams, this means that any correlated pair of tick marks on their respective timelines may be drawn at any point on their timelines provided the two tick marks remain synchronized and proper time ordering is maintained on both timelines. The strength of the term represented by a given FTC diagram is determined by the ability of its constituent pair correlators (segments) to *accumulate* over the response function envelopes for the two timelines. This concept is illustrated by Fig. 1, which shows several examples from the set of FTC diagrams in Table III.

The topology of a given diagram becomes very important when considering accumulation. Notice in Table III that there are three basic topologies manifest in this set of FTC diagrams. Columns ai and bi all have two intrachannel correlations. Columns aii and bii have “crossed” interchannel topology, where the first action (tick mark) on the t timeline is correlated with the second action on the s timeline and vice versa. Finally, columns aiii and biii have “uncrossed” interchannel topology, where the first and second actions on the t timeline are correlated with the first and second actions on the s timeline respectively. Topologically, accumulation is represented by the ability of a tick mark (or in this case, a correlated pair of tick marks) to “slide along the timeline.”

For the intrachannel FTC diagrams (columns ai and bi, there is full and independent accumulation over the “ t_2 interval” i.e., the interval from the second tick mark to the end of the timeline). We will generally refer to the interval from the second tick mark forward in time as the “ t_2 interval” regardless of which channel we are referring to. Likewise, we will refer to the interval between the tick marks as the “ t_1 interval” regardless of channel. The t timeline pair accumulates independently from the s timeline pair [Fig. 1(a)]. However, no accumulation occurs over the t_1 interval. In contrast, the uncrossed FTC diagrams have correlated accumulation over both the t_1 and t_2 intervals. The t timeline and the s timeline accumulation are not independent of one another [Fig. 1(c)]. Finally, the crossed FTC diagrams are the most topologically constrained. Here, full-correlated accumulation can take place over the t_2 interval, but only confined correlated accumulation takes place over the t_1 interval. This confined accumulation will be treated more explicitly in the discussion of indirect correlation.

C. Indirect correlation

With the concepts of synchronization and accumulation in hand, one is in position to understand the interesting phe-

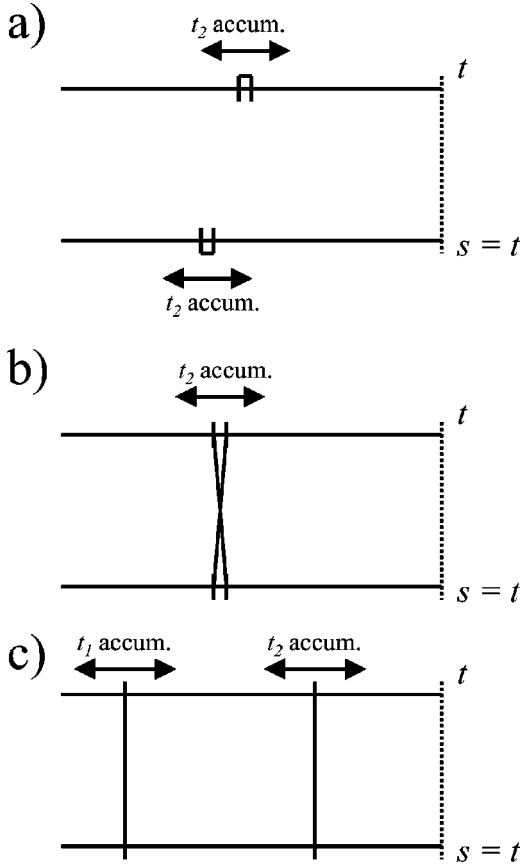


FIG. 1. Illustration of accumulation for each of the three basic topologies of the FTC diagrams: (a) intrachannel, (b) interchannel crossed, and (c) interchannel uncrossed. The dashed vertical line on the right-most side of the FTC diagram is present to emphasize the case when $t=s$, which is used for simplicity in the text. FTC diagrams for the more general case when $t \neq s$ are presented in Appendix B. (a) For the intrachannel FTC diagrams, the two tick marks are synchronized by the δ -function correlation of the random inputs. The two tick marks on each of the timelines are drawn with a slight separation to aid the eye. Actually, they would be superimposed on one another for this diagram. The two tick marks on each timeline cannot change their relative position—they are “locked” together as a correlated pair. So the t_1 interval (between the tick marks) is not accumulated over. However, the correlated pair can “slide along the timeline” as a unit. Thus, the relative position of the pair with respect to the end of the timeline can change. The full t_2 interval on the t timeline, and independently, on the s timeline is accumulated over. (b) The crossed FTC diagrams have a more confined topology. Since the first tick mark on the t timeline is correlated with the second on the s timeline and vice versa, all four tick marks must be coincident. So, no accumulation over the t_1 interval is allowed. Furthermore, accumulation over the t_2 interval does not occur independently on the two channels. (c) For the uncrossed FTC diagrams, the first tick mark on the t timeline is correlated with the first on the s timeline; similarly for the second tick marks. Thus, the relative position of the first and second tick marks can vary. This allows for accumulation over the t_1 interval, where the accumulation is synchronized with the t_1 interval accumulation on the s timeline. Synchronized accumulation also occurs over the t_2 interval.

nomenon of indirect correlation that arises in this second-order/second-order example. The basic principle behind the ability of twin stochastic perturbative driving functions to probe system dynamics is that the stochastic function is impressed upon the system. That is, the system “remembers” this stochastic function such that it can facilitate delayed correlation with the twin stochastic function. The “memory” of the first function fades on the order of the decay of the system response function. This provides a mechanism for extracting the system response function information. Direct correlation of the first and second interaction times (t'_1 and t'_2 or s'_1 and s'_2) is only available to the diagrams of columns ai and bi in Table III. It is clear that these intrachannel correlations will provide response function information by the mechanism just mentioned. The remaining diagrams (columns aii, aiii, bii, and biii) appear, at first glance, to be useless for obtaining response function information because there is no direct correlation between t'_1 and t'_2 or s'_1 and s'_2 . This is not the case, however, because the first and second interaction times on a given timeline are indirectly correlated. Generally, indirect correlation is a consequence of the direct correlation of interchannel pairs of tick marks and the topological constraints of the given FTC diagram. That is, one interaction time (a tick mark on the FTC diagram) on channel 1 is directly correlated to an interaction time on channel 2. The other interaction time on channel 2 is topologically constrained to occur either only before or only after (depending on the FTC diagram) this interaction. The other interaction is in turn directly correlated with the remaining interaction on channel 1. In this roundabout (or *indirect*) way the two intrachannel interactions on channel 1 (and the two on channel 2) are indeed correlated and these types of FTC diagrams can provide response function information. For concreteness we consider two examples.

As a first example, consider FTC diagram T_{VlaIII} as shown in Fig. 2. The two arrowed segments representing these τ -dependent pair correlators do not intersect (interchannel uncrossed segment topology). In this particular example, the first interaction (tick mark) on channel 1 is directly correlated with the first interaction on channel 2 and the second interaction on channel 1 is directly correlated with the second interaction on channel 2. The topological constraints of this FTC diagram forbid the arrowed segments representing the direct correlations from crossing. This imposes a certain behavior on the term represented by this FTC diagram that allows one to obtain response function information through indirect correlation as we shall now see. When the time displacement τ is zero, as in Fig. 2(a), there is full (synchronized) accumulation over the response functions of both channels resulting in the maximal value for the term represented by this diagram. When $\tau > 0$ [Fig. 2(b)], synchronization forces the two tick marks on the s timeline apart by at least 2τ , thus limiting the accumulation over the response function of channel 2 during the t_1 interval. Full accumulation remains available over the t_2 interval on the s timeline. Additionally, accumulation is limited over the t_2 interval on channel 1, but full accumulation is available over the t_1 interval. The value of the term represented by the FTC diagram is necessarily less than that when $\tau=0$. Similarly for $\tau < 0$,

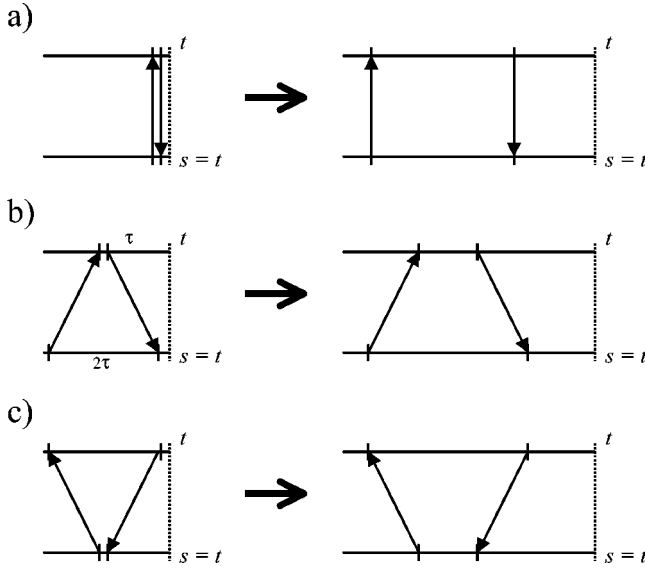


FIG. 2. Indirect correlation in uncrossed FTC diagrams. (a) When $\tau=0$, the first tick mark on the t timeline is exactly coincident with the first tick mark on the s timeline; similarly for the second tick marks. So the arrow segments are drawn vertically (and could, in fact, be replaced with line segments). Full synchronized accumulation occurs over both the t_1 and t_2 intervals. (b) For $\tau > 0$, the first tick mark on the t timeline is now displaced by a magnitude τ from the first tick mark on the s timeline; similarly, but oppositely, for the second tick marks. This means that the two tick marks on the s timeline can come no closer than 2τ apart. Likewise, the second tick marks on the t timeline can come no closer than τ away from the end of the timeline. Therefore, accumulation over both the t_1 and t_2 intervals is diminished compared to when $\tau=0$. (c) For $\tau < 0$, the situation is very similar to when $\tau > 0$, however, now the two tick marks on the t timeline are forced to be at least 2τ apart and the second tick mark on the s timeline is at least τ away from the end of the timeline. So, one generally expects a decrease in the strength of the term represented by uncrossed FTC diagrams as $|\tau|$ is increased.

the two tick marks on the t timeline are forced apart by at least 2τ [Fig. 2(c)]. Now the roles of channel 1 and channel 2 are opposite that of the $\tau > 0$ case. When $|\tau|$ is large enough that the response function of channel 1 or 2 has fully decayed, the value of the term represented by the FTC diagram vanishes.

Now consider FTC diagram T_{vbii} as shown in Fig. 3. Here, the two arrowed segments representing these τ -dependent pair correlators cross each other (crossed segment topology). In this particular example, the first interaction on channel 1 is correlated to the second interaction on channel 2 and the second interaction on channel 1 is correlated to the first interaction on channel 2. The topological constraints of this FTC diagram require that the arrowed segments representing direct correlations remain crossed. When the time displacement τ is zero [Fig. 3(a)] there is necessarily no accumulation (under our approximation of a δ -function time correlator) over the t_1 interval for both channels. This results in a value of zero for the term represented by this FTC diagram. When $\tau < 0$, preservation of the proper time ordering of the samplings forbids any synchronization since

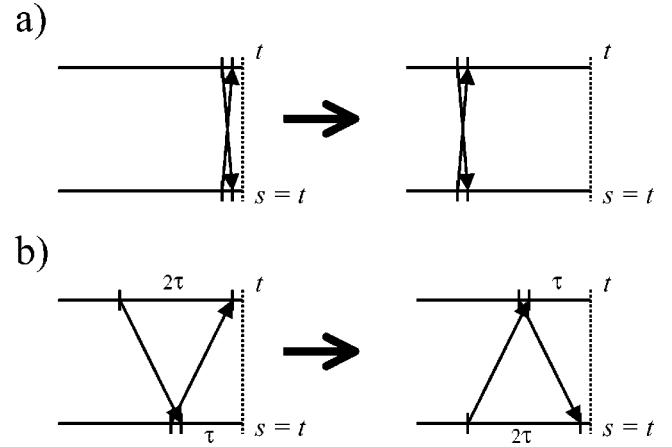


FIG. 3. Indirect correlation in crossed FTC diagrams. (a) When $\tau=0$, this case is exactly equivalent to the τ independent crossed FTC diagrams (line segments only) and so the value of the term represented by the diagram is zero. (b) For $\tau > 0$, the topological constraint is relaxed as the tick marks on both the t timeline and s timeline can now move relative to one another by up to 2τ . This allows for some accumulation over the t_1 interval. Full accumulation is available over the t_2 interval. So, one generally expects the contribution from crossed FTC diagrams to initially increase with increasing $|\tau|$.

the two correlated pairs of tick marks can never be simultaneously synchronized. This also produces a zero value for the term represented by this FTC diagram for $\tau < 0$. On the other hand, for $\tau > 0$ [Fig. 3(b)], synchronization of both of the pair correlators can be simultaneously satisfied. Now accumulation over the t_1 interval is limited to no more than 2τ on both the t and s timelines. However, unlike accumulation in the uncrossed case, separation of tick marks on the t timeline forces the tick marks on the s timeline closer together and vice versa. So, there are two basic ways indirect correlation is manifest in this two-channel system: (i) tick marks are forced apart by at least some τ -dependent interval (not necessarily 2τ) for the uncrossed segment topology or (ii) the tick marks are confined to be no more than some τ -dependent interval apart as for the crossed segment diagrams.

V. FTC DIAGRAM ANALYSIS

The general ideas of FTC diagram analysis discussed above can now be applied to the current system such that a mapping is made from the FTC diagrams to the general solution for this second-order/second-order case. A very common situation is the case where $t=s$ (e.g., homodyne detection in spectroscopy and light intensity in optics). We shall work with this case simply as a matter of convenience. The situation where $t \neq s$ poses no fundamental problem but the FTC diagram analysis becomes unnecessarily clouded by the additional complication. FTC diagram analysis for the case where $t \neq s$ is briefly addressed in Appendix B by way of example.

There are two important properties of the signal that can be obtained immediately from the set of FTC diagrams. The first property is τ symmetry. For the set of FTC diagrams in

TABLE IV. The general expressions for the FTC diagrams having intrachannel topology (columns ai and bi of Table III).

Term	$\tau > 0$	$\tau < 0$
T_{Iai}	$\int_0^\infty dt_2 \int_0^\infty ds_2 R_1(t_2; 0) R_2(s_2; 0)$	$\int_0^\infty dt_2 \int_0^\infty ds_2 R_1(t_2; 0) R_2(s_2; 0)$
T_{Ibi}	$\int_0^\infty dt_2 \int_0^\infty ds_2 R_1(t_2; \tau) R_2(s_2; 0)$	0
T_{IIai}	0	$\int_0^\infty dt_2 \int_0^\infty ds_2 R_1(t_2; -\tau) R_2(s_2; 0)$
T_{IIbi}	$\int_0^\infty dt_2 \int_0^\infty ds_2 R_1(t_2; 0) R_2(s_2; 0)$	$\int_0^\infty dt_2 \int_0^\infty ds_2 R_1(t_2; 0) R_2(s_2; 0)$
T_{IIIai}	0	$\int_0^\infty dt_2 \int_0^\infty ds_2 R_1(t_2; 0) R_2(s_2; -\tau)$
T_{IIIbi}^a	0	0
T_{IVai}	0	$\int_0^\infty dt_2 \int_0^\infty ds_2 R_1(t_2; -\tau) R_2(s_2; -\tau)$
T_{IVbi}	0	$\int_0^\infty dt_2 \int_0^\infty ds_2 R_1(t_2; 0) R_2(s_2; -\tau)$
T_{Vai}	$\int_0^\infty dt_2 \int_0^\infty ds_2 R_1(t_2; 0) R_2(s_2; \tau)$	0
T_{Vbi}	$\int_0^\infty dt_2 \int_0^\infty ds_2 R_1(t_2; \tau) R_2(s_2; \tau)$	0
T_{VIai}^a	0	0
T_{VIbi}	$\int_0^\infty dt_2 \int_0^\infty ds_2 R_1(t_2; 0) R_2(s_2; \tau)$	0
T_{VIIai}	$\int_0^\infty dt_2 \int_0^\infty ds_2 R_1(t_2; 0) R_2(s_2; 0)$	$\int_0^\infty dt_2 \int_0^\infty ds_2 R_1(t_2; 0) R_2(s_2; 0)$
T_{VIIbi}	$\int_0^\infty dt_2 \int_0^\infty ds_2 R_1(t_2; \tau) R_2(s_2; 0)$	0
T_{VIIIai}	0	$\int_0^\infty dt_2 \int_0^\infty ds_2 R_1(t_2; -\tau) R_2(s_2; 0)$
T_{VIIIbi}	$\int_0^\infty dt_2 \int_0^\infty ds_2 R_1(t_2; 0) R_2(s_2; 0)$	$\int_0^\infty dt_2 \int_0^\infty ds_2 R_1(t_2; 0) R_2(s_2; 0)$

^aPrecisely at $\tau=0$ these terms are equivalent to T_{Iai} . The discontinuity is a consequence of the δ -function correlation function for the random input functions.

Table III, one sees that each diagram is paired with another with respect to inversion of the direction of the arrow; for example T_{Ibi} and T_{IIai} or T_{IIIbii} and T_{VIaiii} , etc. From the topology of the FTC diagrams, for this second order/second-order case, the signal must be a symmetric function of τ regardless of the choice of response function. One might have expected general τ symmetry from the structure of the driving force, i.e., the roles of F and F' should be symmetric. While the present second-order/second-order case did indeed turn out to yield a signal that was symmetric in τ , this cannot always be assumed for general n_1^{th} -order/ n_2^{th} -order cases. The original work using FTC diagram analysis and the very same driving function to model a degenerate four-wave mixing process in nonlinear optical spectroscopy, which is of the third-order/third-order type, shows an asymmetric signal [4].

A second property is the dynamic range or peak to background contrast ratio. This is simply the ratio of $\langle A_2^{(2)}(s, \tau = 0) A_1^{(2)}(t, \tau = 0) \rangle$ to $\langle A_2^{(2)}(s, \tau \rightarrow \infty) A_1^{(2)}(t, \tau \rightarrow \infty) \rangle$. Considering the set of FTC diagrams in Table III, one sees that 12 of the 48 diagrams are τ -independent (lines only). Of these 12 diagrams, there are three types (intrachannel, interchannel crossed, and interchannel uncrossed) each having a fourfold degeneracy. Now, considering the full set of FTC diagrams, at $\tau=0$ all the arrows in the τ -dependent diagrams can be drawn as lines. Again, there are three types, but now the degeneracy is 16 (including the τ -independent diagrams). As $\tau \rightarrow \infty$, all the arrowed diagrams vanish. Thus, the peak to background contrast ratio is 16:4 or 4:1. Like the τ symmetry, this is independent of the choice of the response function. Also like the τ symmetry, other cases such as third-order/third-order examples can exhibit different peak-to-background contrast ratios than for this second-order/second-order case.

Now one can apply the principles of FTC diagram analysis to obtain the general analytic structure of the terms represented by the diagrams. Turning first to the intrachannel FTC diagrams of columns ai and bi in Table III, we have stated that full and independent accumulation is available over the t_2 intervals on both channels. Analytically, this statement implies that two separate integrations must be performed. Furthermore, no integration is done over the t_1 intervals. So the general analytic structure of the intrachannel FTC diagrams is

$$\int_0^\infty dt_2 \int_0^\infty ds_2 R_1(t_2; x) R_2(s_2; y), \quad (15)$$

where x and y are 0 for line segments, τ ($-\tau$) for arrows pointing to the right (left) and $\tau > 0$ ($\tau < 0$). The value of the term represented by the FTC diagram is zero when at least one arrow points to the right (left) and $\tau < 0$ ($\tau > 0$). The results for all the intrachannel diagrams are listed in Table IV.

For the crossed FTC diagrams we know, from the general discussion in the previous section, that at most a given diagram will represent a term having a nonzero value for either $\tau > 0$ or $\tau < 0$. Correlated accumulation is available over the t_2 intervals. The accumulation is limited, however, over the t_1 interval. Thus, the analytic structure of these diagrams (when the terms they represent are not equal to zero) is

$$\int_0^\infty dt_2 \int_0^u dt_1 R_1(y_1; t_1) R_2(y_2; x), \quad (16)$$

where $u = \pm \tau$ or $\pm 2\tau$, $x = u - t_1$ and y_1 and y_2 are appropriate time arguments (too varied to conveniently summarize here). The results for each of the crossed FTC diagrams are listed in Table V.

TABLE V. General expressions for the crossed FTC diagrams (columns aii and bii of Table III). To condense the table, let $T_{21} \equiv t_2 + t_1$ and $t_{21} \equiv t_2 - t_1$.

Term	$\tau > 0$	$\tau < 0$
T_{Iaii}	0	0
T_{Ibii}	$\int_0^\infty dt_2 \int_0^\tau dt_1 R_1(t_2; t_1) R_2(T_{21}; \tau - t_1)$	0
T_{IIaii}	0	$\int_0^\infty dt_2 \int_0^{-\tau} dt_1 R_1(t_{21} - \tau; t_1) R_2(t_2; -\tau - t_1)$
T_{IIbii}	0	0
T_{IIIaii}	0	$\int_0^\infty dt_2 \int_0^{-\tau} dt_1 R_1(t_2; t_1) R_2(T_{21}; -\tau - t_1)$
T_{IIIbii}	0	0
T_{IVaii^a}	0	$\int_0^\infty dt_2 \int_0^{-2\tau} dt_1 R_1(t_2; t_1) R_2(T_{21} + \tau; -2\tau - t_1)$
T_{IVbii}	0	$\int_0^\infty dt_2 \int_0^{-\tau} dt_1 R_1(t_{21} - \tau; t_1) R_2(t_2; -\tau - t_1)$
T_{Vaii}	$\int_0^\infty dt_2 \int_0^\tau dt_1 R_1(t_{21} + \tau; t_1) R_2(t_2; \tau - t_1)$	0
T_{Vbii^a}	$\int_0^\infty dt_2 \int_0^{2\tau} dt_1 R_1(t_2; t_1) R_2(T_{21} - \tau; 2\tau - t_1)$	0
T_{VIaii}	0	0
T_{VIbii}	$\int_0^\infty dt_2 \int_0^\tau dt_1 R_1(t_2; t_1) R_2(T_{21}; \tau - t_1)$	0
T_{VIIaii}	0	0
T_{VIIbii}	$\int_0^\infty dt_2 \int_0^\tau dt_1 R_1(t_{21} + \tau; t_1) R_2(T_2; \tau - t_1)$	0
T_{VIIIaii}	0	$\int_0^\infty dt_2 \int_0^{-\tau} dt_1 R_1(t_2; \tau_1) R_2(T_{21}; -\tau - t_1)$
T_{VIIIbii}	0	0

^aCausality of the response functions was used to simplify the expression to a single term. FTC diagram analysis would more naturally give

$$\int_0^\infty dt_2 \int_0^{\pm\tau} dt_1 R_1(t_{21} \pm \tau; t_1) R_2(t_2; \pm 2\tau - t_1) + \int_0^\infty dt_2 \int_{\pm\tau}^{\pm 2\tau} dt_1 R_1(t_2; t_1) R_2(T_{21} \mp \tau; \pm 2\tau - t_1).$$

Uncrossed FTC diagrams have correlated accumulation over the t_1 and t_2 intervals. For these diagrams, it is most convenient to associate the accumulation with full integration from zero to infinity over both the t_1 and t_2 intervals. In doing this, however, one must account for the limitations of the accumulation by appropriately choosing the arguments of the response function. So the general analytic structure of the uncrossed FTC diagrams is

$$\int_0^\infty dt_2 \int_0^\infty dt_1 R_1(x_1; y_1) R_2(x_2; y_2), \quad (17)$$

where $x_1, y_1, x_2,$ and y_2 are the appropriate time arguments; too varied to conveniently summarize here, but the explicit expressions for each of the uncrossed FTC diagrams are collected in Table VI.

The most natural way to analyze FTC diagrams is to treat

TABLE VI. General expressions for the uncrossed FTC diagrams of Table III (columns aiii and biii).

Term	$\tau > 0$	$\tau < 0$
T_{Iaiii}	$\int_0^\infty dt_2 \int_0^\infty dt_1 R_1(t_2; t_1) R_2(t_2; t_1)$	$\int_0^\infty dt_2 \int_0^\infty dt_1 R_1(t_2; t_1) R_2(t_2; t_1)$
T_{Ibiii}	$\int_0^\infty dt_2 \int_0^\infty dt_1 R_1(t_2; t_1 + \tau) R_2(t_2 + \tau; t_1)$	$\int_0^\infty dt_2 \int_0^\infty dt_1 R_1(t_2 - \tau; t_1) R_2(t_2; t_1 - \tau)$
T_{IIaiii}	$\int_0^\infty dt_2 \int_0^\infty dt_1 R_1(t_2; t_1) R_2(t_2; t_1 + \tau)$	$\int_0^\infty dt_2 \int_0^\infty dt_1 R_1(t_2; t_1 - \tau) R_2(t_2; t_1)$
T_{IIbiii}	$\int_0^\infty dt_2 \int_0^\infty dt_1 R_1(t_2; t_1) R_2(t_2 + \tau; t_1)$	$\int_0^\infty dt_2 \int_0^\infty dt_1 R_1(t_2 - \tau; t_1) R_2(t_2; t_1)$
T_{IIIaiii}	$\int_0^\infty dt_2 \int_0^\infty dt_1 R_1(t_2; t_1 + \tau) R_2(t_2; t_1)$	$\int_0^\infty dt_2 \int_0^\infty dt_1 R_1(t_2; t_1) R_2(t_2; t_1 - \tau)$
T_{IIIbiii}	$\int_0^\infty dt_2 \int_0^\infty dt_1 R_1(t_2; t_1 + 2\tau) R_2(t_2 + \tau; t_1)$	$\int_0^\infty dt_2 \int_0^\infty dt_1 R_1(t_2 - \tau; t_1) R_2(t_2; t_1 - 2\tau)$
T_{IVaiii}	$\int_0^\infty dt_2 \int_0^\infty dt_1 R_1(t_2; t_1) R_2(t_2; t_1)$	$\int_0^\infty dt_2 \int_0^\infty dt_1 R_1(t_2; t_1) R_2(t_2; t_1)$
T_{IVbiii}	$\int_0^\infty dt_2 \int_0^\infty dt_1 R_1(t_2; t_1 + \tau) R_2(t_2 + \tau; t_1)$	$\int_0^\infty dt_2 \int_0^\infty dt_1 R_1(t_2 - \tau; t_1) R_2(t_2; t_1 - \tau)$
T_{Vaiii}	$\int_0^\infty dt_2 \int_0^\infty dt_1 R_1(t_2 + \tau; t_1) R_2(t_2; t_1 + \tau)$	$\int_0^\infty dt_2 \int_0^\infty dt_1 R_1(t_2; t_1 - \tau) R_2(t_2 - \tau; t_1)$
T_{Vbiii}	$\int_0^\infty dt_2 \int_0^\infty dt_1 R_1(t_2; t_1) R_2(t_2; t_1)$	$\int_0^\infty dt_2 \int_0^\infty dt_1 R_1(t_2; t_1) R_2(t_2; t_1)$
T_{VIaiii}	$\int_0^\infty dt_2 \int_0^\infty dt_1 R_1(t_2 + \tau; t_1) R_2(t_2; t_1 + 2\tau)$	$\int_0^\infty dt_2 \int_0^\infty dt_1 R_1(t_2; t_1 - \tau) R_2(t_2 - \tau; t_1)$
T_{VIbiii}	$\int_0^\infty dt_2 \int_0^\infty dt_1 R_1(t_2; t_1) R_2(t_2; t_1 + \tau)$	$\int_0^\infty dt_2 \int_0^\infty dt_1 R_1(t_2; t_1 - 2\tau) R_2(t_2; t_1)$
T_{VIIaiii}	$\int_0^\infty dt_2 \int_0^\infty dt_1 R_1(t_2 + \tau; t_1) R_2(t_2; t_1)$	$\int_0^\infty dt_2 \int_0^\infty dt_1 R_1(t_2; t_1) R_2(t_2 - \tau; t_1)$
T_{VIIbiii}	$\int_0^\infty dt_2 \int_0^\infty dt_1 R_1(t_2; t_1 + \tau) R_2(t_2; t_1)$	$\int_0^\infty dt_2 \int_0^\infty dt_1 R_1(t_2; t_1) R_2(t_2; t_1 - \tau)$
T_{VIIIaiii}	$\int_0^\infty dt_2 \int_0^\infty dt_1 R_1(t_2 + \tau; t_1) R_2(t_2; t_1 + \tau)$	$\int_0^\infty dt_2 \int_0^\infty dt_1 R_1(t_2; t_1 - \tau) R_2(t_2 - \tau; t_1)$
T_{VIIIbiii}	$\int_0^\infty dt_2 \int_0^\infty dt_1 R_1(t_2; t_1) R_2(t_2; t_1)$	$\int_0^\infty dt_2 \int_0^\infty dt_1 R_1(t_2; t_1) R_2(t_2; t_1)$

TABLE VII. Expressions for the specific example of the response function described in Eq. (19).

Term	i	ii	iii
Ia	$\frac{1}{g^2}$	0	$\frac{1}{4g}$
Ib	$\frac{e^{-T}}{g^2}$	$\frac{e^{-T}T}{2g}$	$\frac{e^{-(1+g)T}}{4g}$
IIa	0	0	$\frac{e^{-2T}}{4g}$
IIb	$\frac{1}{g^2}$	0	$\frac{e^{-gT}}{4g}$
IIIa	0	0	$\frac{e^{-T}}{4g}$
IIIb	0	0	$\frac{e^{-(2+g)T}}{4g}$
IVa	0	0	$\frac{1}{4g}$
IVb	0	0	$\frac{e^{-(1+g)T}}{4g}$
Va	0	$\frac{e^{-T}T}{2g}$	$\frac{e^{-(1+g)T}}{4g}$
Vb	$\frac{e^{-2T}T}{g^2}$	$\frac{e^{-2T}T}{g}$	$\frac{1}{4g}$
VIa	$\frac{e^{-T}}{g^2}$	0	$\frac{e^{-(2+g)T}}{4g}$
VIb	$\frac{e^{-T}}{g^2}$	$\frac{e^{-T}T}{2g}$	$\frac{e^{-2T}}{4g}$
VIIa	$\frac{1}{g^2}$	0	$\frac{e^{-gT}}{4g}$
VIIb	$\frac{e^{-T}}{g^2}$	$\frac{e^{-T}T}{2g}$	$\frac{e^{-T}}{4g}$
VIIIa	0	0	$\frac{e^{-(1+g)T}}{4g}$
VIIIb	$\frac{1}{g^2}$	0	$\frac{1}{4g}$

the $\tau > 0$ and $\tau < 0$ cases separately. The direct analytical calculation of the terms associated with the diagrams does not naturally treat the cases separately. At first glance, it is not obvious that the two results are equivalent. In fact, for noncausal response functions, they are not equivalent, but FTC diagrams are not valid in noncausal situations. The equivalence of these two methods of obtaining the final form of the expressions is shown in Appendix A. One nice feature of the form of the expression arising from FTC analysis is that causality is automatically built in. So, when an explicit form of the response function is chosen, one need not explicitly include the step function as a factor in the response function. This is beneficial when evaluating particular cases using computer algebra software such as MATHEMATICA to auto-

mate the process. The disadvantage of the FTC diagram approach is that each diagram has two cases: $\tau > 0$ and $\tau < 0$. This is compounded when considering the more general situation when $t \neq s$ (see Appendix B).

It is interesting to investigate how each of the different terms represented by FTC diagrams probe the response functions. As stated above, the intrachannel FTC diagrams (columns ai and bi of Table III) directly probe the response functions; more precisely, the response during the t_1 interval. Since full accumulation is always available over the t_2 interval, it cannot be probed as a function of τ . Diagrams T_{Ibi} , T_{IIai} , T_{VIIbi} , and T_{VIIIai} isolate the t_1 interval for channel 1. Diagrams T_{IIIai} , T_{IVbi} , T_{Vai} , and T_{VIbi} isolate the t_1 interval for channel 2. Finally, diagrams T_{IVai} and T_{Vbi} simultaneously probe channel 1 and 2. All the crossed FTC diagrams isolate the t_1 interval but not independently on each channel. Only the uncrossed FTC diagrams are capable of probing the t_2 interval. Diagrams T_{IIbii} and $T_{VIIaiii}$ isolate the t_2 interval. Furthermore, for $\tau > 0$ diagram T_{IIbii} isolates t_2 on channel 1 and diagram $T_{VIIaiii}$ isolates t_2 on channel 2. (For $\tau < 0$, the roles of these diagrams are reversed.) Diagrams T_{Ibiii} , $T_{IIIbiii}$, T_{IVbiii} , T_{Vaiii} , T_{VIaiii} , and $T_{VIIIaiii}$ simultaneously probe the t_1 and t_2 intervals.

A. Example

As an example, consider the system in which the response functions are

$$R_1(t_2; t_1) = \Theta(t_1)\Theta(t_2)e^{-\gamma_1 t_1}e^{-\gamma_2 t_2}, \quad (18)$$

$$R_2(s_2; s_1) = \Theta(s_1)\Theta(s_2)e^{-\gamma_1 s_1}e^{-\gamma_2 s_2}.$$

(Note: both channel 1 and channel 2 have identical response functions which we simply call R .) Since causality is automatically included in the FTC diagram derived expressions, one can drop the step-function factors. Furthermore, the response function can be nondimensionalized by working in units of, say, γ_1 and defining $T_i = \gamma_1 t_i$, $g = \gamma_2 / \gamma_1$. Then,

$$R = e^{-T_1}e^{-gT_2}. \quad (19)$$

The expressions for each of the FTC diagrams for $\gamma_1 \tau = T > 0$ are listed in Table VII. It is interesting to consider the relative strengths of the different topologies of the diagrams. The intrachannel diagrams (column i of Table VII) are proportional to $1/g^2$, the crossed diagrams (column ii) are proportional to T/g and the uncrossed diagrams (column iii) are proportional to $1/g$. Considering the crossed diagrams first, one sees that the expressions go to zero as $T \rightarrow 0$ as generally expected from the principles of FTC diagram analysis. Now, considering the intrachannel and uncrossed diagrams, the ratio of the uncrossed to intrachannel terms is $(1/g)/(1/g^2) = g = \gamma_2 / \gamma_1$. So we see that if $\gamma_2 > \gamma_1$, the uncrossed terms dominate, whereas if $\gamma_2 < \gamma_1$ the intrachannel terms dominate. This is what is expected from the standpoint of accumulation. The intrachannel diagrams have two full accumulations over the t_2 interval, whereas the uncrossed diagrams have one accumulation each over the t_1 and t_2 intervals. So if the decay of the response is faster during the t_2 interval

($\gamma_2 > \gamma_1$) then one expects the intrachannel diagrams to be disadvantaged. Conversely, if the decay is slower ($\gamma_2 < \gamma_1$) the intrachannel diagrams have the advantage of greater total accumulation.

VI. CONCLUSION

In this paper, the properties and mathematical structure of factorized time correlation (FTC) diagram analysis were examined in a generalized context. That is, the general principles and analytic behavior were not explicitly or implicitly tied to any particular phenomenon in physics (other than driven causal systems). The specific case of second order/second order was used as the working example in order to give a concreteness to the general principles and procedures of FTC diagram analysis. It was shown that the topological structure of the FTC diagrams yields much information about the signal as a function of τ such as symmetry, dynamic range, and general analytic structure of the terms the diagrams represent. The very interesting phenomenon of indirect correlation was presented. The FTC diagrams provided a topological interpretation of this phenomenon that is readily seen. It is hoped that this paper will provide a basis for expanded use of FTC diagram analysis. Currently, FTC diagram analysis has only been exploited in the study of noisy light-based nonlinear optical spectroscopy. Expansion of its use into other areas of physics could provide very beneficial cross fertilization of ideas and deepened insight into these areas.

ACKNOWLEDGMENTS

The authors wish to express much appreciation to Jahan Mansoor Dawlaty and Sam MacDonald for valuable discussions. We also are indebted to Mustafa M. Rajabali for pointing out an error in one of our tables that we were able to correct.

APPENDIX A

In the text, it was noted that FTC diagram analysis yields expressions in a different from than what naturally arises from the direct analytical calculation. In this Appendix, we show the equivalence of these two methods of obtaining the final expression. As in the text, we take as the example term $T_{V\text{Ia}iii}$

Beginning with Eq. (13), we consider the two cases $\tau > 0$ and $\tau < 0$ and the situation where $s = t$ (Appendix B addresses the more general case of $s \neq t$). One now must specifically invoke the causal nature of R . This implies

$$T_{V\text{Ia}iii} = \int_{\tau}^{\infty} dt_2 \int_0^{\infty} dt_1 R_1(t_2; t_1) R_2(t_2 - \tau; t_1 + 2\tau), \quad \tau > 0 \quad (\text{A1})$$

(n.b., the lower limit of the t_2 integration can be set to τ) and

$$T_{V\text{Ia}iii} = \int_0^{\infty} dt_2 \int_{-2\tau}^{\infty} dt_1 R_1(t_2; t_1) R_2(t_2 - \tau; t_1 + 2\tau), \quad \tau < 0 \quad (\text{A2})$$

(n.b., the lower limit of the t_1 integration can be set to -2τ). With a simple change of variables one can write

$$T_{V\text{Ia}iii} = \begin{cases} \int_0^{\infty} dt_2 \int_0^{\infty} dt_1 R_1(t_2 + \tau; t_1) R_2(t_2; t_1 + 2\tau), & \tau > 0 \\ \int_0^{\infty} dt_2 \int_0^{\infty} dt_1 R_1(t_2; t_1 - 2\tau) R_2(t_2 - \tau; t_1), & \tau < 0 \end{cases}, \quad (\text{A3})$$

which agrees precisely with the expression obtained from FTC diagram analysis (Table VI).

APPENDIX B

Throughout the discussion of FTC diagram analysis, the simplified case of $s = t$ was used. This was a convenience rather than a necessity. In this Appendix, the case of $s \neq t$ is briefly addressed by way of an example, namely, term $T_{V\text{Ia}iii}$. From a direct calculation standpoint, the case when $s \neq t$

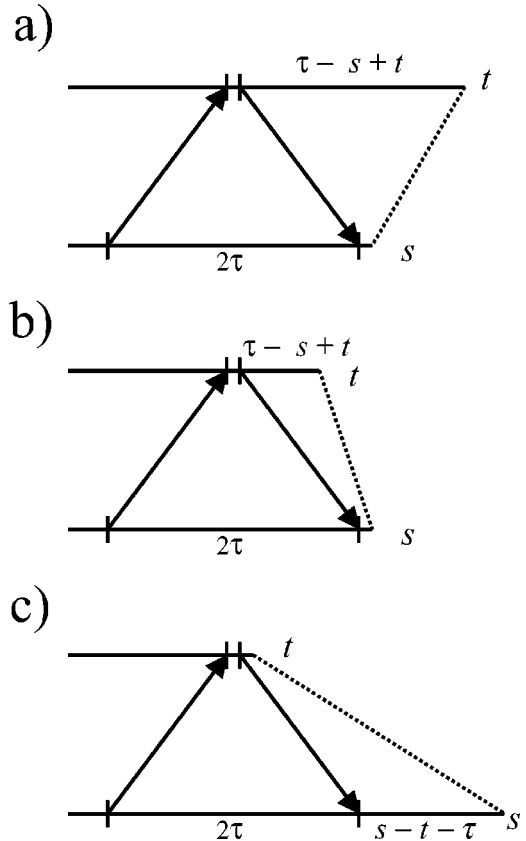


FIG. 4. FTC diagram $T_{V\text{Ia}iii}$ for the case when $t \neq s$ and $\tau > 0$. (a), (b) $s - t < \tau$. Here, the accumulation over the t_2 interval on channel 1 is restricted in that the second tick mark on the t timeline can be no closer to the end of the timeline than $\tau - s + t$. Full accumulation over the t_2 interval on channel 2 is allowed. (c) $s - t < \tau$. In this case, full accumulation is allowed over the t_2 interval on channel 1 but is restricted on channel 2. The second tick mark on the s timeline can be no closer than $s - t - \tau$ from the end of the timeline.

does not need to be treated in any special manner. It arises naturally as in Eq. (13). From a FTC diagram standpoint, however, $s \neq t$ has topological significance. Direct prediction of the expression represented by the diagrams involves considering two cases for $\tau > 0$ and two cases for $\tau < 0$. We shall focus on $\tau > 0$ for FTC diagram T_{Vlaaiii} . Here, one must consider the case when $s - t < \tau$ and the case when $s - t > \tau$. Figure 4 illustrates these two cases. Figures 4(a) and 4(b) are both cases when $s - t < \tau$. One sees that the accumulation over the t_2 interval on the t timeline is effected by $s \neq t$. Since τ exceeds $s - t$, accumulation over the t_2 interval on the s timeline remains full. Thus, one predicts, for $s - t < \tau$ and $\tau > 0$,

$$T_{\text{Vlaaiii}} = \int_0^\infty dt_2 \int_0^\infty dt_1 R_1(t_2 + \tau - s + t; t_1) R_2(t_2; t_1 + 2\tau). \quad (\text{B1})$$

Figure 4(c) shows the case where $s - t > \tau$. In this case, full accumulation can take place over the t_2 interval in the t timeline, but accumulation over that same interval on the s timeline is diminished. So, for the $s - t > \tau > 0$ situation one predicts

$$T_{\text{Vlaaiii}} = \int_0^\infty dt_2 \int_0^\infty dt_1 R_1(t_2; t_1) R_2(t_2 + s - t - \tau; t_1 + 2\tau). \quad (\text{B2})$$

As with the $s = t$ case, the collection of expressions can be shown to be equivalent to Eq. (13) by explicitly considering the causal nature of R and making simple changes of variables as was done in Appendix A.

-
- [1] A. M. Yaglom, *Correlation Theory of Stationary and Related Random Functions I: Basic Results* (Springer-Verlag, New York, 1987).
- [2] N. Wiener, *Nonlinear Problems in Random Theory* (Wiley, New York, 1958).
- [3] R. Deutsch, *Nonlinear Transformations of Random Processes* (Prentice Hall, Englewood Cliffs, NJ, 1962).
- [4] D. J. Ulness and A. C. Albrecht, Phys. Rev. A **53**, 1081 (1996).
- [5] J. C. Kirkwood, A. C. Albrecht, D. J. Ulness, and M. J. Stimson, Phys. Rev. A **58**, 4910 (1998).
- [6] J. C. Kirkwood and A. C. Albrecht, Phys. Rev. A **61**, 033802 (2000).
- [7] J. C. Kirkwood and A. C. Albrecht, Phys. Rev. A **61**, 043803 (2000).
- [8] M. Pfeiffer and A. Lau, J. Chem. Phys. **108**, 4159 (1998).
- [9] D. J. Ulness and A. C. Albrecht, J. Raman Spectrosc. **28**, 571 (1997).
- [10] D. J. Ulness and A. C. Albrecht, J. Raman Spectrosc. **28**, 579 (1997).
- [11] L. Mandel and E. Wolf, *Optical Coherence and Quantum Optics* (Cambridge University, New York, 1995).
- [12] J. W. Goodman, *Statistical Optics* (Wiley, New York, 1985).
- [13] C. L. Mehta, in *Lectures in Theoretical Physics*, edited by W. E. Britin (University of Colorado, Boulder, CO, 1965), Vol. VII C.